Desalination and Water Treatment
www.deswater.com

doi: 10.1080/19443994.2015.1101022

57 (2016) 19519–19528
September

Taylor & Francis
Taylor & Francis Group

Removal of manganese ions from their aqueous solutions by organophilic montmorillonite (OMMT)

A.A. Bakr[a,*], M.A. Betiha[b], A.H. Mady[c], M.F. Menoufy[b], S.M. Dessouky[b]

[a]*Department of Analysis and Evaluation, Egyptian Petroleum Research Institute (EPRI), Nasr City, Cairo 11727, Egypt, Tel. +20 1227135228; email: als_water@yahoo.com*
[b]*Department of Refining, Egyptian Petroleum Research Institute (EPRI), Nasr City, Cairo 11727, Egypt, Tel. +20 1112815390; email: mohamed_betiha@hotmail.com (M.A. Betiha), Tel. +20 1223614989; email: mohamedfathyh@yahoo.com (M.F. Menoufy), Tel. +20 1223508118; email: usdesouky@yahoo.com (S.M. Dessouky)*
[c]*Department of Petrochemicals, Egyptian Petroleum Research Institute (EPRI), Nasr City, Cairo 11727, Egypt, Tel. +20 1112724232; email: amr_mady@yahoo.com*

Received 27 March 2015; Accepted 22 September 2015

ABSTRACT

This paper deals with the organophilic montmorillonite (OMMT) which was used as the manganese ions adsorbent from the aqueous solutions. This organoclay nanocomposite was synthesized by cation exchange of Na-MMT with 12-aminolauric acid (ALA) and denoted as ALA-MMT. The acidic montmorillonite (H-MMT) was prepared by cation exchange of Na-MMT with 2.0 N hydrochloric acid. The synthesized materials were characterized by X-ray diffraction analysis, Fourier transform infrared spectroscopy analysis, Transmission electron microscopy analysis, Scanning electron microscopy analysis, and Thermogravimetric analysis. The adsorption behavior was studied at ambient temperature, stirring rate of 160 rpm, different solution pH values (2–9), different contact times (15–150 min), different initial Mn(II) concentrations (30–100 mg/L), and different adsorbent masses (0.2–0.55 g per 1.0 L). At the optimum conditions of the initial Mn(II) concentration of 100 mg/L, solution pH 6, adsorbent mass of 0.35 g/L and contact time of 90 min, the results revealed that the maximum adsorption capacities were 15.3 and 9.3 mg/g for OMMT and H-MMT, respectively, while at adsorbent mass of 0.55 g/L, the maximum adsorption capacities reached 28.6 and 17.3 mg/g for OMMT and H-MMT, respectively. Therefore, particularly, the solution pH range of 5–7 has the most significant effect on the adsorption capacity and the organoclay nanocomposite materials could act as a highly effective adsorbents for Mn(II) from the aqueous solutions.

Keywords: Water treatment; Organophilic montmorillonite (OMMT); Organoclay nanocomposite; Mn(II) adsorption

1. Introduction

Manganese can be found in natural waters in its most reduced and soluble form (the Mn(II) ion) and in the oxide form (MnO_2; pyrolusite), respectively. If not oxidized, Mn(II) ions can easily escape through water treatment processes and can gradually be oxidized to insoluble manganic dioxide (MnO_2) in the distribution systems causing several problems such as

*Corresponding author.

water discoloration, metallic taste, odor, turbidity, biofouling, corrosion, and staining of laundry and plumbing fixture [1]. For high intake manganese having adverse neurotoxic health effect, World Health Organization (WHO) recommends guideline value of 0.4 mg/L to protect against neurological damage [2]. European Union (EU) and the Environmental Protection Agency (EPA) have established the level of 0.05 mg/L for manganese [3,4]. So, if concentrations are higher than these standards, water must be treated before using it for drinking purposes. The excessive concentrations of Mn will result in a metallic taste in water, staining of different products like clothes, paper, and plastics [5]. Manganese can also cause build up in pipelines, water heaters, and pressure tanks. The deposition of manganese in the distribution systems can cause diameter reduction of pipes and eventually clogging of pipes will take place [6].

Oxidation and precipitation are the most common methods to remove Mn(II). Such method is based on the Mn(II) oxidation to its insoluble manganic dioxide, followed by clarification and/or filtration. Manganic dioxide is also found to adsorb the manganese ion which can be progressively oxidized with time [7]. Encouraging results for manganese removal have also been obtained by GAC adsorption [8] and biological processes [9,10], with removal up to 95%. Nano-adsorbents are quite efficient for the fast adsorption of heavy-metal ions and organic molecules from aqueous solutions with regard to their high specific surface areas and absence of internal diffusion resistance [11].

Previously, the clays and clay minerals have been demonstrated as adsorbents for the removal of heavy metals [12–15]. While, the low loading capacity, relatively small metal ion binding, and low metal selectivity of these materials are inherent stable [16,17]. So, to overcome these limitations, the clay minerals were modified with ligands containing metal-chelating groups in different studies. The modification of the clay minerals takes place with organic molecules such as intercalation, impregnation, ion exchange, and grafting. These organoclays have been demonstrated to be good adsorbents for toxic metals such as Cr, Pb, Cd, Hg, and Zn [16,18,19]. Thereafter, the modified organic montmorillonites (organo-Mts) have been demonstrated to be good adsorbents for heavy metals [20].

The removal of manganese, cadmium, zinc, and chromium from aqueous systems were studied by a clay mineral and their maximum adsorption capacity was 0.52 mmol/g of Mn^{2+} [21]. The adsorption capacities for Hg(II) by 2-(3-(2-aminoethylthio)propylthio)- ethanamine (AEPE)-montmorillonite and AEPE-hectorite were 46.1 and 54.7 mg/g, respectively, for solution containing 140 mg/L Hg(II) ions [20]. The maximum adsorption capacity of Th(IV) on magnetic organo-bentonite-Fe_3O_4 poly-(sodiumacrylate) at pH 3.0 ± 0.05 and T = 298 K was about 6.55 mmol/g [22]. In this study, the resulted experiments showed that the maximum adsorption capacity of organophilic montmorillonite (OMMT) was 28.6 mg/g, and this value is much larger than those in a previous study of Ca-MMT, sodium dodecyl sulfate (SDS)-MMT and hexadecyl trimethyl ammonium bromide (HDTMAB)-MMT (13.23, 26.85, and 3.91 mg/g, respectively) [23].

The objectives of the present study are synthesis of OMMT, applying this organoclay nanocomposite material for Mn(II) removal from aqueous solutions, determining the adsorption rate and capacity, and therefore, studying the initial solution pH, adsorbent mass, effect of contact time, and effect of initial Mn(II) concentration. Thereafter, we prospect the mechanism of Mn(II) removal.

2. Materials and methods

2.1. Materials

Sodium MMT clay (Na-MMT) was supplied by Kunimine Industry under the trade name Kunipia-F with a cation-exchange capacity (CEC) of 119 mEq/100 g. 12-aminolauric acid (ALA, 95%), hydrochloric acid (37%), silver nitrate (99%)and manganese chloride ($MnCl_2{\cdot}4H_2O$) were purchased from Loba chemie Co.

2.2. Preparation of OMMT

OMMT was prepared by cation exchange of Na-MMT with ALA [24,25]. Surface alteration of MMT by ALA hydrochloride was carried out as follows; ALA chloride solution was prepared by the addition of 2.0 g of concentrated HCl (0.2 mol) to 4.3 g of ALA (0.2 mmol) in 300 ml of distilled water. The mixture was stirred at 65˚C for 1.0 h to form a clear solution. To this solution, pre-swelled Na-MMT (10 g of Na-MMT in 250 ml of distilled water) was added dropwise at room temperature under mechanical stirring for 4.0 h, and then, the temperature rose to 80˚C for 5.0 h. The obtained fine white aggregates were collected by suction filtration and re-stirred in methanol–water mixture (50:50, V:V) several times until chloride-free ions were detected by 0.1 N $AgNO_3$ in the filtrate. The resulted white material was air dried, ground in mortar, and finally sieved. The organoclay was denoted as ALA-MMT.

2.3. Preparation of acidic montmorillonite

Aquaphobia Na-MMT was prepared by cation exchange of Na-MMT with 2.0 N hydrochloric acid. Specifically, 50 mL of 2.0 N HCl was added dropwise to pre-swelled Na-MMT (5.0 g in 25 mL distilled water). The resulting mixture was centrifuged and the precipitated acidic MMT was redispersed in 100 mL of toluene. This step was repeated two additional times to remove the unbound NaCl molecules.

2.4. Characterization of prepared materials

2.4.1. X-ray diffraction analysis

X-ray diffraction patterns were performed on Pan Analytical Model X′ Pert Proinstrument with CuKa ($\lambda = 0.154$ nm) radiation. The diffractograms were recorded in the 2θ range of 4–80 degree with a two-step size of 0.01˚ and a step time of 10 s.

2.4.2. Fourier transform infrared spectroscopy analysis

Fourier transform infrared spectroscopy analysis (FT-IR) spectra of the pure materials and adsorbed samples were carried out using an ATI Unicam (Mattson 936) spectrometer.

2.4.3. Transmission electron microscopy analysis

Transmission electron microscopy (HRTEM) images were obtained using a JEOL 2011 electron microscope (Japan) and operated at 200 kV.

2.4.4. Scanning electron microscopy analysis

The morphology of the samples was investigated using a field-emission scanning electron microscope (FESEM, S4800).

2.4.5. Thermogravimetric analysis

Thermal stability was carried out in a TA Instruments SDT Q600 simultaneous Thermogravimetric analysis (TGA)–DSC thermogravimetric analyzer.

2.5. Adsorption method

The manganese stock solution with a concentration of 500 mg/L was prepared by dissolving $MnCl_2{\cdot}4H_2O$ in distilled water. The working Mn(II) solution concentration, ranging from 30 to 100 mg/L for all experiments was freshly prepared from the stock solution. Standard acid (0.01 M HNO_3) and base solutions (0.125 M NaOH) were used for pH adjustments at pH 2, 2.5, 3, 4, 5, 6, 7, 8, 8.5, and 9. The pH of solution was measured with a pH meter (Thermo Orion 5 Star) using a combined glass electrode (Orion 81–75). The pH meter was calibrated with buffers of pH 4.0 and 7.0 before any measurement.

The experiments for the removal of manganese ions from dilute aqueous solutions by the addition of adsorbent masses (OMMT and acidic montmorillonite (H-MMT)) of 0.20, 0.25, 0.30, 0.35, 0.40, 0.45, 0.50, and 0.55 g/L were carried out at temperature 298 k, using distilled water and conical flasks (100 mL sample volume). After continuous stirring over a magnetic stirrer at about 160 rpm for predetermined time intervals (15, 30, 45, 60, 75, 90, 105, 120, 135, and 150 min), the solid and solution were separated by centrifugation at 3,000 rpm for 15 min, and slightly dried at ambient temperature. Mn(II) concentration was determined by Spectrophotometer (UV–vis), LaMotte, model SMART Spectro, USA and the solid phase was analyzed. The contact time allows the dispersion of adsorbent and metal ions to reach equilibrium conditions, as found during preliminary experiments.

2.6. Calculations

The amount of adsorption q_e (mg/g) and the percentage of removal were calculated by the following equations [26,27]:

$$q_e = \frac{V(C_o - C_e)}{m} \tag{1}$$

$$\text{Adsorption}\,(\%) = \frac{(C_o - C_e)}{C_o} \times 100 \tag{2}$$

where C_o and C_e are the initial Mn(II) concentration and the concentration at equilibrium in mg/L, m is the mass of the adsorbent, and V is the volume of the solution.

2.7. Effect of initial solution pH

The effect of initial solution pH on Mn(II) removal was evaluated by making a series of 100 mg/l manganese ions solutions at an adsorbent dosage of 0.35 g/l, the starting solution pH values were adjusted to the designed values at ambient temperature and contact time 90 min. The prepared OMMT and H-MMT suspensions were filtered, and then, the residual of Mn(II) concentrations were analyzed.

2.8. Effect of adsorbent mass

Different masses of the prepared OMMT and H-MMT were added to a series of 100 ml of Mn(II) solutions with initial concentration of 100 mg/l at pH 6.0, stirring rate 160 rpm for constant contact time 90 min and at ambient temperature to reach the equilibrium. Then, the aqueous samples were filtered and then, the residual Mn(II) concentrations were analyzed.

3. Results and discussion

3.1. Characterization of ALA-MMT and H-MMT

3.1.1. X-ray diffraction analysis

Fig. 1(A) shows the LXRD patterns of Na-MMT and ALA-MMT. The Na-MMT and ALA-MMT patterns reveal the characteristic diffraction peaks at 7.12° and 5.05°, respectively, corresponding to basal spacing (d_{001}) of 1.24, 1.76 nm, respectively. Thus, OMMT exhibited a larger basal spacing than Na-MMT. This could be associated with the intercalation of the alkyl ammonium chains into galleries of MMT. Fig. 1(B) shows the collapse of layer after replacing Na^+ by proton due to the removal of water form interlayers (diffraction at 7.12° shifted to 9.09°). The ALA-MMT showed a considerable widening of the X-ray diffraction analysis (XRD) peaks and loss of intensity due to less ordering of MMT layers. In addition, the *d*-spacing of ALA-MMT increased after Mn^{2+} adsorption due to the more solubility of $(–COO)_2$ Mn group.

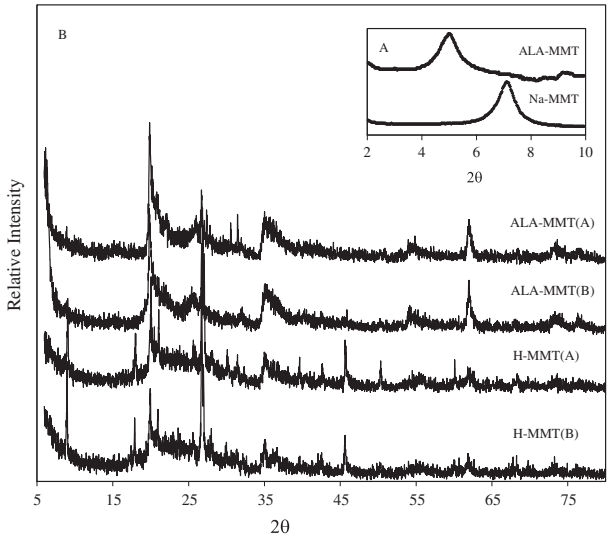

Fig. 1. XRD patterns of (A) LXAD of H-MMT and ALA-MMT and (B) H-MMT and ALA-MMT before and after Mn(II) adsorption.

The reflections in the pattern could be clearly indexed based on a monoclinic cell reported for manganese chelated oxygen atom, JCPDS No. 41-1442, Mn_2O_3 and JCPDS No. 80-0382, Mn_3O_4, for ALA-MMT and H-MMT, respectively.

3.1.2. Fourier transform infrared spectroscopy analysis

The FTIR data of pristine H-MMT and ALA-MMT are presented in Fig. 2. The characteristic bands of H-MMT are shown by stretching and bending hydroxyl group, Si–O in-plane stretching, as well as Al–O/Al–OH stretching vibrations, which were observed at ≈3,470, 1,648, 1,052, and 924 cm^{-1}, respectively. The bands below 800 cm^{-1} at 839, 693, and 613 cm^{-1} were assigned to Si–O deformation, Al–MgOH deformation, and coupled Al–O and Si–O vibration [28]. The characteristic absorption peaks of ALA were also found at 3,672 (–OH stretching), 2,939 ($–CH_3$ stretching), 2,863 ($–CH_2$ stretching), 1,643 (O–H bending), 1,552 cm^{-1} ($–CH_2$ stretching), and N–H deformation, as well as C–N stretching absorptions, respectively. It is noted that the FTIR spectrum of the OMMT shows the combination of characteristic bands of the pure MMT and the ALA, demonstrating the successful organic modification of Na-MMT. After adsorption of Mn^{2+}, both bands at 3,673 and 924 cm^{-1} is diminished for ALA-MMT (after) and H-MMT due to Mn^{2+} incorporation, respectively [28].

3.1.3. Transmission electron microscopy analysis

The morphology of H-MMT (B) and ALA-MMT (B) (Fig. 3) was identical to H-MMT (A) and ALA-MMT (A), indicating that the layer structures of MMT were intact deposited Mn^{2+} on the surface of

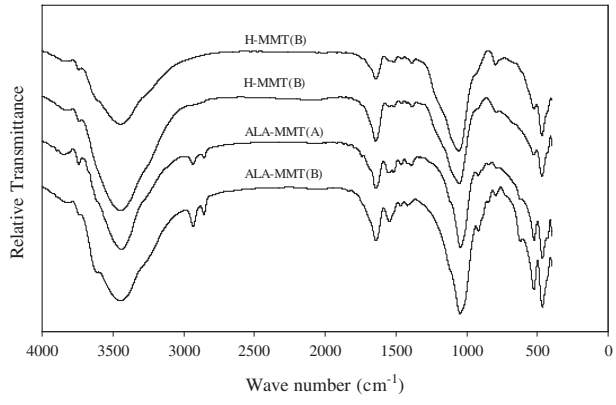

Fig. 2. FTIR spectra of ALA-MMT and H-MMT before and after Mn(II) adsorption.

the MMT layers. Bright-field TEM images showed a large amorphous region between matrix and darker regions, and in the peripheral region were lamellar structures [29]. As shown in Fig. 3, manganese ions were well dispersed on ALA-MMT, while clear and clean MMT layers were also observed. The distribution of Mn^{2+} in H-MMT was less than ALA-MMT due to the incorporation of Mn^{2+} on the surface and inside MMT layers.

3.1.4. Scanning electron microscopy analysis

As indicated in Fig. 4, the morphology of the H-MMT and ALA-MMT materials before and after adsorption showed clear differences: the layer sheets of the ALA-MMT consisted of a higher number of stacking layer compared with the H-MMT. The layer sheets were exfoliated and became thinner after adsorption, as a result of the strong hydrophilic nature of Mn^{2+} complex. After adsorption, the Mn/MMT materials exhibited higher dispersion in water than the H-MMT because of the thinner layer sheets of the former.

3.1.5. Thermogravimetric analysis

The TGA curves of Na-MMT and ALA-MMT are shown in Fig. 5. ALA-MMT showed weight loss

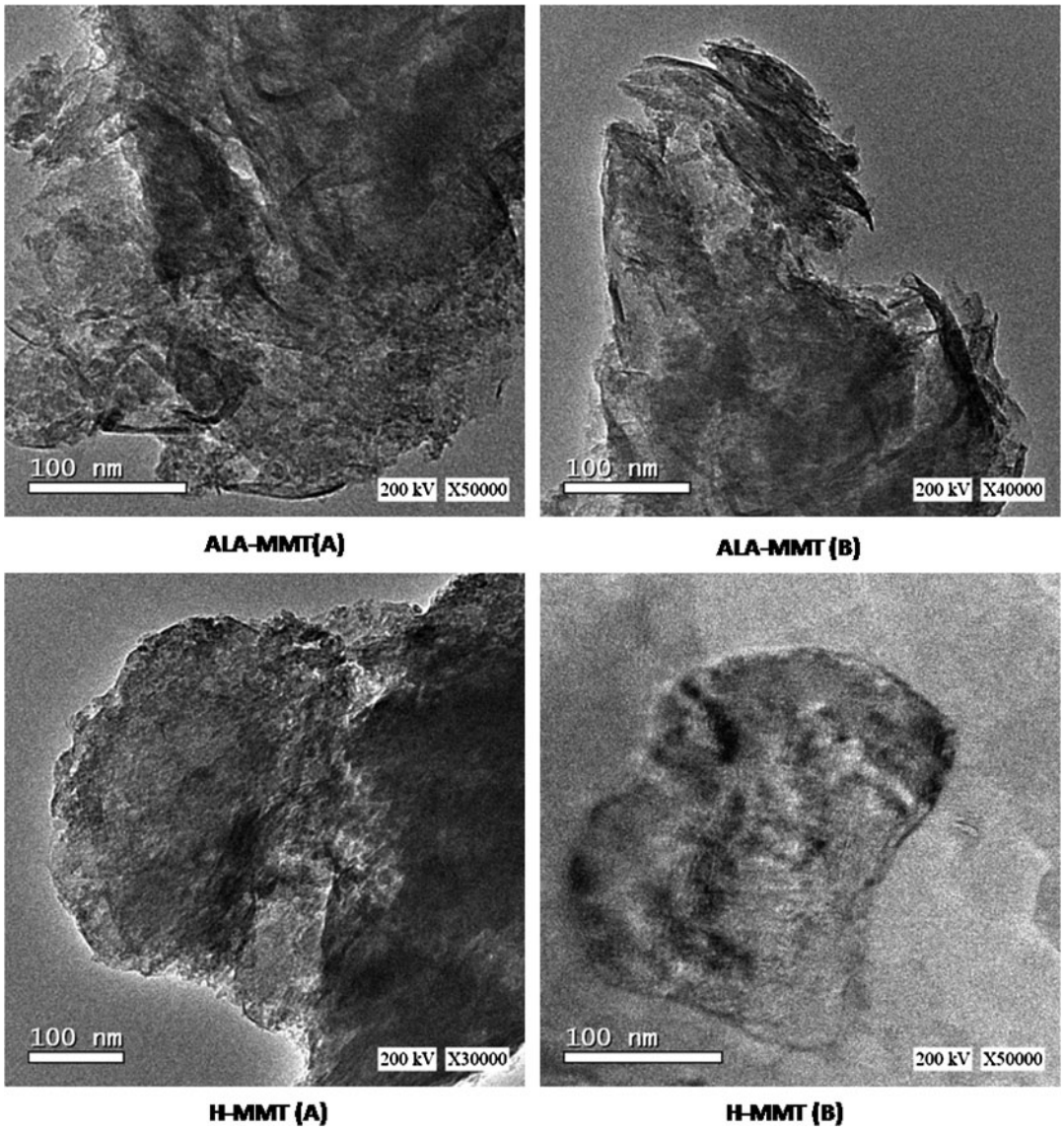

Fig. 3. HRTEM of ALA-MMT and H-MMT before and after Mn(II) adsorption.

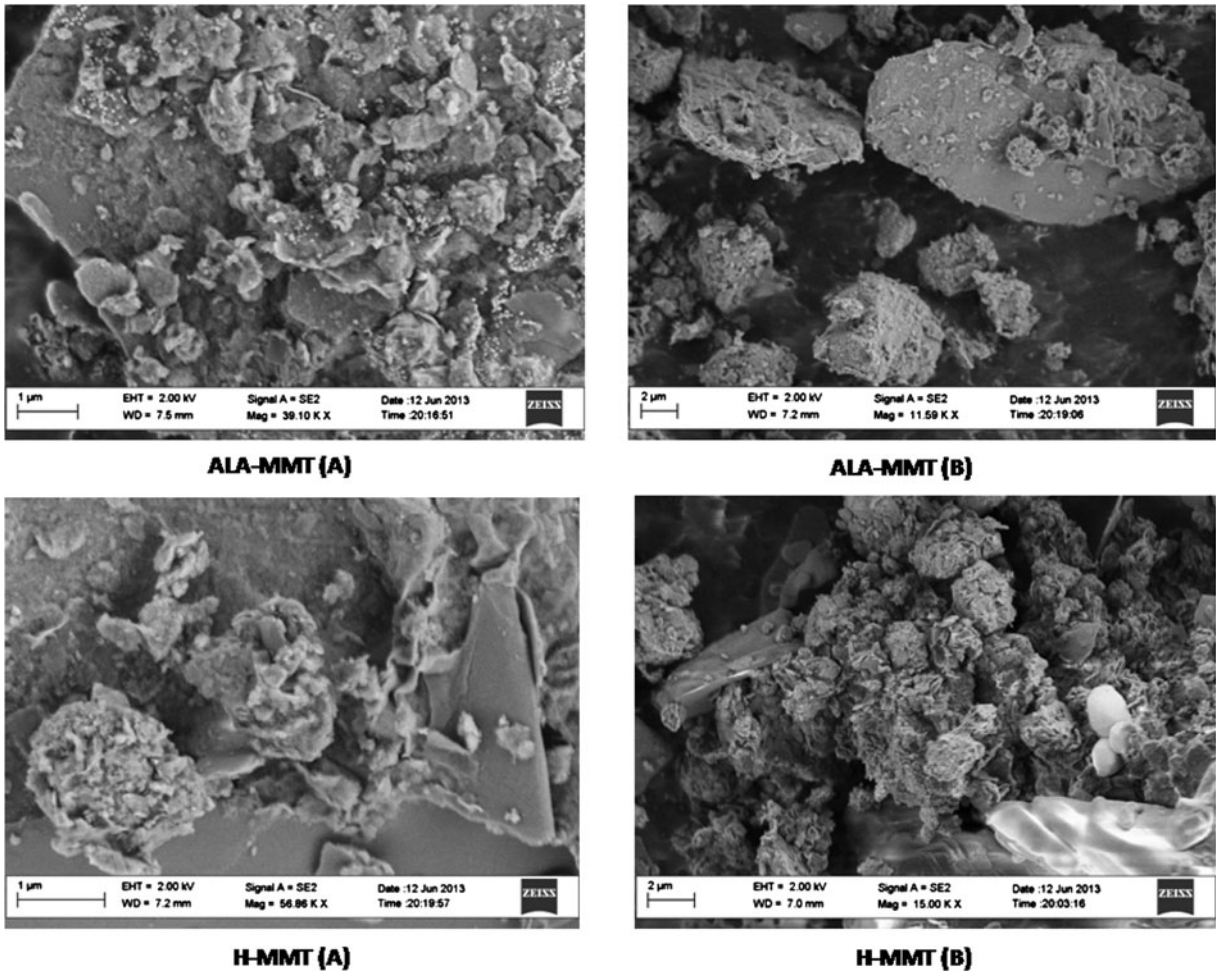

Fig. 4. FESEM of ALA-MMT and H-MMT before and after Mn(II) adsorption.

relatively higher than that of H-MMT, corresponding to the removal of ALA hydrochloride from interlayers. The H-MMT showed higher weight loss than ALA-MMT below 100°C, due to the removal of water coordinated to Na^+. The weight loss in the temperature regime of 100–600°C is due to the decomposition of hydrogen-bonded water molecules and some of the OH group from tetrahedral sheets, and in the temperature range of 600–750°C, the weight losses for H-MMT and ALA-MMT were probably associated with the dehydroxylation of H-MMT [30].

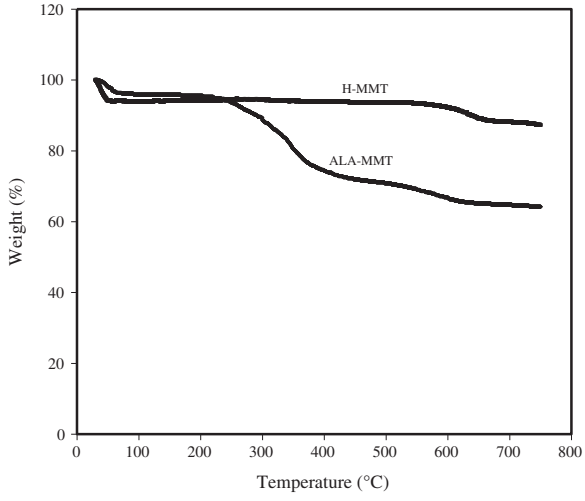

Fig. 5. TGA curves of H-MMT and ALA-MMT.

3.2. Initial solution pH

The effect of starting solution pH on the removal % of Mn(II) from solutions with an initial concentrations of 100 mg/L on 0.35 g/L of OMMT and H-MMT after 90 min is shown in Fig. 6. The data indicated that the amounts of Mn(II) adsorbed on ALA-MMT and

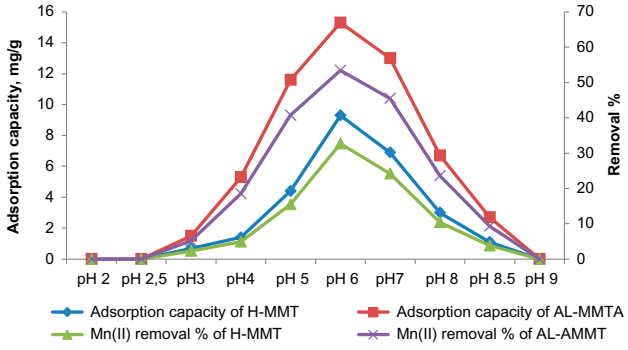

Fig. 6. Effect of initial solution pH on the removal percentage and adsorption capacity of H-MMT and ALA-MMT materials (initial Mn(II) concentration 100 mg/l, temperature 298˚C, adsorbent mass 0.35 g/l, stirring rate 160 rpm, contact time 90 min).

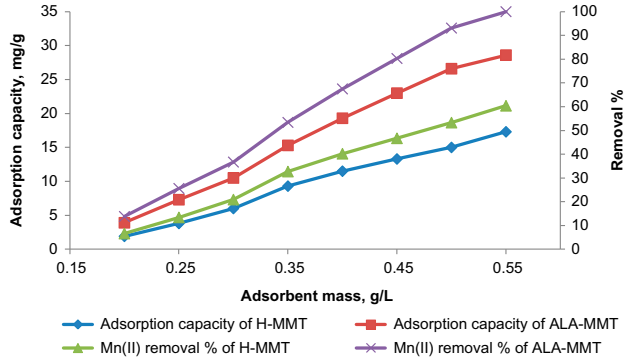

Fig. 7. Adsorbent masses as a function of Mn(II) removal percentage and adsorption capacity of H-MMT and ALA-MMT materials (initial concentration 100 mg/l, temperature 298˚C, pH 6.0, stirring rate 160 rpm, contact time 90 min).

H-MMT decreased with decreasing pH for a starting solution pH ≤ 4, while for pH > 4, the removal seems to be pH-independent.

From Fig. 6, at above pH 4, adsorption capacities increased with increasing pH values, and reached to its maximum value at pH 6 and then slowly decreased. Then, the adsorption decreased and appeared to reach a plateau in the pH range of ≥7. At pH 6 and temperature 298 k, the adsorption capacities of Mn(II) on OMMT and H-MMT were 15.3 and 9.3 mg/g, then slowly decreased at pH 7.0 to 13.0 and 6.9 mg/g, respectively while, at higher pH value of 9.0, the adsorption capacities were sharply decreased to 0.0 and 0.0 mg/g at pH 9, respectively.

In a previous study, the adsorption of metal ions on bentonite was strongly dependent on pH, which indicated that the ion exchange and/or outer-sphere complexes were the main adsorbed species at low pH, and inner-sphere and/or surface precipitation complexes dominated at high pH [31].

3.3. Adsorbent mass

At ambient temperature, the different dosages of ALA-MMT and H-MMT were added to a series of 100 mL of Mn(II) solutions with initial concentration of 100 mg/L at pH 6.0 and stirring rate of 160 rpm for contact time 90 min to reach the equilibrium. Then, the aqueous samples were filtered, and then the residual Mn(II) concentrations were analyzed. The effect of the adsorbent mass on the Mn(II) adsorption in 100 mg/L solutions is shown in Fig. 7. For these experiments, the metal solutions containing the appropriate adsorbent dose were loaded in 100 mL snap-seal polyethylene bottles, which were then stirred at 160 rpm for 105 min. The mixture in each bottle was then centrifuged immediately, and the Mn(II) concentrations in the supernatant solutions were determined by Spectrophotometer. Fig. 7 represents that the first removal percentage and adsorption capacity of Mn(II) increased sharply with increasing the adsorbent dosage, which may be due to the improvement of surface complexation capacity with increasing adsorbent concentration [22,32]. At the optimum dose of 0.35 g/L, the removal % were 53.4 and 32.7 for ALA-MMT and H-MMT, respectively, and with increasing the adsorbent dosage to 0.55 g/L, the removal % for H-MMT was 60.4 and the removal % reached 100 for ALA-MMT.

3.4. Equilibrium time

Fig. 8 shows the effect of contact time required to reach the equilibrium on the adsorption capacity and removal % of 100 mg/L of initial Mn(II) concentration onto 0.35 g/L of OMMT and H-MMT at pH 6, stirring rate of 160 rpm, and temperature, 298 k. It can be seen from Fig. 8 that the adsorption rate was considerably fast within the first 30 min, the removal % were 23.9 and 20.7 for ALA-MMT and H-MMT, respectively, then gradually increased at 90 min, when the removal % were 53.4 and 32.7 for OMMT and H-MMT, respectively, and thereafter, the removal percentage reached 100 in case of OMMT, while it reached only 34.5 in case of H-MMT at 150 min.

The initial rapid adsorption may be due to the increased number of the available sites at the initial stage. So, the increase in the concentration gradient tends to increase the Mn(II) adsorption rate within the initial 30 min. As the time proceeded, the concentration

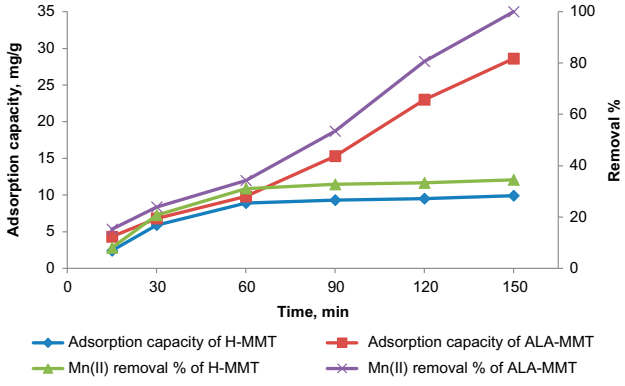

Fig. 8. Effect of contact time on the removal percentage and adsorption capacity of H-MMT and ALA-MMT materials (initial Mn(II) concentration 100 mg/l, temperature 298˚C, adsorbent mass 0.35 g/l, pH 6.0, stirring rate 160 rpm).

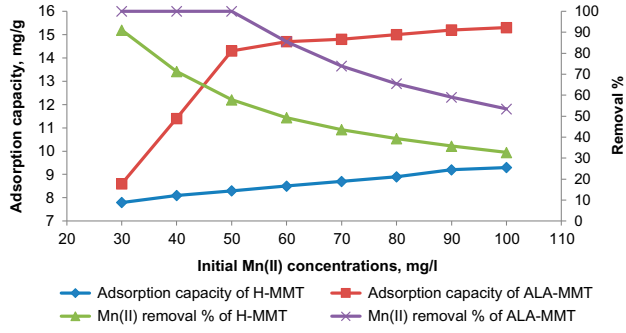

Fig. 9. Effect of initial Mn(II) concentration on the removal percentage and adsorption capacity of H-MMT and ALA-MMT materials (temperature 298˚C, adsorbent mass 0.35 g/l, pH 6.0, stirring rate 160 rpm, contact time 90 min).

gradients became reduced owing to the accumulation of more than 5.9 and 6.8 mg of Mn(II) adsorbed per gram of H-MMT and ALA-MMT surface sites after 30 min, leading to the adsorption capacities of 9.3 and 15.3 mg/g after 90 min and then at the later time (150 min), the adsorption capacities became 9.9 and 28.6 mg/g, respectively.

The fast Mn(II) removal rate in the beginning is attributed to the rapid diffusion of Mn(II) from the solution to the external surfaces of H-MMT and OMMT and also attributed to the longer diffusion range of Mn(II) into the inner-sphere of adsorbent or the ion-exchange in the inner surface. Such slow diffusion will lead to a slow increase in the adsorption curve at later stages [33].

3.5. Initial adsorbate concentration

The effect of different Mn(II) concentrations was determined after experimental studies which were carried out for a range of metal concentrations. A definite dosage of adsorbent (H-MMT and OMMT, 0.35 g/L) was added to a series of 100 mL of Mn(II) solutions with different initial concentrations of 30, 40, 50, 60, 70, 80, 90, and 100 mg/L at pH 6.0, and stirring rate of 160 rpm for contact time 90 min to reach the equilibrium.

Fig. 9 indicated that the OMMT apparently removed a considerable amount of Mn(II) from the aqueous solutions. The adsorption capacity increased to a certain level (≤50 mg/L), and saturated beyond a certain concentration (>50 mg/L). Saturation resulted when no more metal ions could be adsorbed on the surface of OMMT where the adsorption occurred.

Also, Fig. 9 showed that high efficiency for Mn(II) adsorption could be obtained over a relatively short period of up to 90 min. The removal of initial Mn(II) concentrations exhibited that the removal amounts were linearly proportional to the initial metal concentrations. However, the complete removals of Mn(II) were observed at initial concentrations 30, 40, and 50 mg/L for OMMT, when the adsorption capacities were 8.6, 11.4, and 14.3 mg/g, respectively, while, only 91.0% from the initial concentration of 30 mg/L for the H-MMT was removed when the adsorption capacity was 7.8 mg/g. Then, the removal percentages increased slowly with increasing the initial Mn(II) concentrations to 100 mg/L for OMMT (53.4%) when the adsorption capacity was 15.3 mg/g and for H-MMT (32.7%) when the adsorption capacity was 9.3 mg/g.

3.6. Mechanism of Mn(II) adsorption

The enhancement of adsorption capacity of clay minerals can be done by replacing the natural exchangeable cations with organic molecules, forming the so-called “organoclays”. This process can render the clay surface more hydrophobic or hydrophilic, at will, depending on the nature of the organic molecule [34]. The adsorption of divalent metal ions (M^{2+}) onto montmorillonite clay usually involves two distinct mechanisms: firstly; an ion-exchange reaction at permanent-charge sites, and, secondly; the formation of complexes with surface hydroxyl groups at edge sites [35–38]. Also, there four novel organo-modified montmorillonites were prepared and tested as sorbent materials for the removal of heavy metals from aqueous solutions and the modification was based on the functionalization of the clay surfaces by various

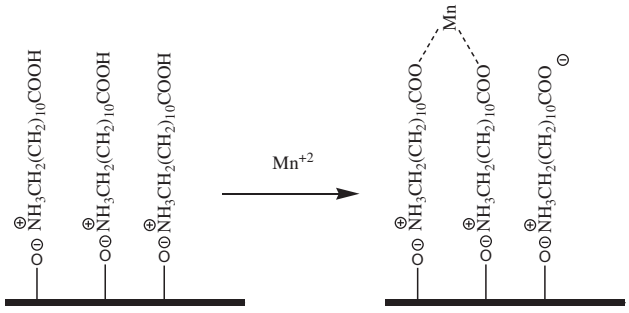

Fig. 10. Schematic drawing of the proposed mechanism of manganese adsorption on ALA-MMT.

chelating groups (–NH_2, –COOH, –SH, and –CS_2) that can effectively capture metal ions [39].

In the present work, the carboxyl-functionalized MMT exhibited unique affinity for manganese ions. It can be seen that ALA-MMT adsorbent efficiently removed the Mn^{2+} ions. Therefore, the concentration changes are indeed attributed to the complexation reactions between manganese ions and grafted carboxyl groups, Fig. 10.

4. Conclusions

The present study showed that the synthesized organoclay nanocomposite and ALA were suitable adsorbents for the Mn(II) removal from aqueous solutions. The characteristics of the synthesized materials were studied using XRD, FT-IR, TEM, Scanning electron microscopy analysis (SEM), and TGA. The optimum adsorption conditions were the initial Mn(II) concentration of 100 mg/L, solution pH value of 6, adsorbent dose of 0.35 gram per liter, and contact time of 90 min with maximum adsorption capacities of 15.3 and 9.3 mg/g for OMMT and H-MMT, respectively, while, at adsorbent mass of 0.55 g/L, the maximum adsorption capacity reached 28.6 mg/g for OMMT. Therefore, the synthesized organoclay nanocomposite and ALA could act as a suitable adsorbents for Mn(II) removal from aqueous solutions and the OMMT material has a higher potential application than the H-MMT product in Mn(II) removal field.

References

[1] P. Roccaro, C. Barone, G. Mancini, F.G.A. Vagliasindi, Removal of manganese from water supplies intended for human consumption: A case study, Desalination 210 (2007) 205–214.
[2] WHO, Guideline for Drinking Water Quality, Health Criteria and Other Supporting Information, 1, third ed., Geneva, (2004).
[3] European Union, Richtlinie 98/83/EG des Rates, (1998).
[4] U.S. EPA. Office of water, National Secondary Drinking Water Regulations, In Code of Federal Regulations, (2001) 612–614.
[5] S.C. Homoncik, A.M. MacDonald, K.V. Heal, B.É.Ó. Dochartaigh, B.T. Ngwenya, Manganese concentrations in Scottish groundwater, Sci. Total Environ. 408 (2010) 2467–2473.
[6] A.G. Tekerlekopoulou, D.V. Vayenas, Ammonia, Iron and manganese removal from potable water using trickling filters, Desalination 210 (2006) 225–235.
[7] A. Voorinen, Chemical, mineralogical, and microbiological factors affecting the precipitation of Fe and Mn from groundwater, Water Sci. Technol. 20 (1988) 249–259.
[8] A.B. Jusoh, W.H. Cheng, W.M. Low, A. Nora'aini, M.J. Megat Mohd Noor, Study on the removal of iron and manganese in groundwater by granular activated carbon, Desalination 182 (2005) 347–353.
[9] V.A. Pacini, A.M. Ingallinella, G. Sanguinetti, Removal of iron and manganese using biological roughing up flow filtration technology, Water Res. 39 (2005) 4463–4475.
[10] I.A. Katsoyiannis, A.I. Zouboulis, Biological treatment of Mn(II) and Fe(II) containing groundwater: Kinetic considerations and product characterization, Water Res. 38 (2004) 1922–1932.
[11] S. Zhang, F. Cheng, Z. Tao, F. Gao, J. Chen, Removal of nickel ions from wastewater by $Mg(OH)_2$/MgO nanostructures embedded in Al_2O_3 membranes, J. Alloys Compd. 426 (2006) 281–285.
[12] S.E. Bailey, T.J. Olin, R.M. Bricka, D.D. Adrian, A review of potentially low-cost sorbents for heavy metals, Water Res. 33 (1999) 2469–2479.
[13] M. Borisover, E.R. Graber, F. Bercovich, Z. Gerstl, Suitability of dye-clay complexes for removal of non-ionic organic compounds from aqueous solutions, Chemosphere 44 (2001) 1033–1040.
[14] R. Naseem, S.S. Tahir, Removal of Pb(II) from aqueous/acidic solutions by using bentonite as an adsorbent, Water Res. 35 (2001) 3982–3986.
[15] M.G. da Fonseca, M.M. de Oliveira, L.N.H. Arakaki, Removal of cadmium, zinc, manganese and chromium cations from aqueous solution by a clay mineral, J. Hazard. Mater. 137 (2006) 288–292.
[16] L. Mercier, C. Detellier, Preparation, characterization, and application as heavy metals sorbents of covalently grafted thiol functionalities on the interlamellar surface of montmorillonite, Environ. Sci. Technol. 29 (1995) 1318–1323.
[17] L. Mercier, T.J. Pinnavaia, Heavy metal ion adsorbents formed by the grafting of a thiol functionality to mesoporous silica molecular sieves: Factors affecting Hg(II) uptake, Environ. Sci. Technol. 32 (1998) 2749–2754.
[18] B.S. Krishna, D.S.R. Murty, B.S.J. Prakash, Surfactant-modified clay as adsorbent for chromate, Appl. Clay Sci. 20 (2001) 65–71.
[19] M. Erdemoğlu, S. Erdemoğlu, F. Sayılkan, M. Akarsu, Ş. Şener, H. Sayılkan, Organo-functional modified pyrophyllite: Preparation, characterisation and Pb(II) ion adsorption property, Appl. Clay Sci. 27 (2004) 41–52.

[20] T. Phothitontimongkol, N. Siebers, N. Sukpirom, F. Unob, Preparation and characterization of novel organo-clay minerals for Hg(II) ions adsorption from aqueous solution, Appl. Clay Sci. 43 (2009) 343–349.
[21] M.G.D. Fonseca, M.M.D. Oliveira, L.N.H. Arakaki, Removal of cadmium, zinc, manganese and chromium cations from aqueous solution by a clay mineral, J. Hazard. Mater. 137 (2006) 288–292.
[22] L. Wu, Y. Ye, F. Liu, C. Tan, H. Liu, S. Wang, J. Wang, W. Yi, W. Wu, Organo-bentonite-Fe_3O_4 poly(sodium acrylate) magnetic superabsorbent nanocomposite: Synthesis, characterization, and Thorium(IV) adsorption, Appl. Clay Sci. 83–84 (2013) 405–414.
[23] P. Wu, Y. Dai, H. Long, N. Zhu, P. Li, J. Wu, Z. Dang, Characterization of organo-montmorillonites and comparison for Sr(II) removal: Equilibrium and kinetic studies, Chem. Eng. J. 191 (2012) 288–296.
[24] A. Rehab, A. Akelah, T. Agag, M. Betiha, Polymer–organoclay hybrids by polymerization into montmorillonite vinyl monomer interlayers, J. Appl. Polym. Sci. 106 (2007) 3502–3514.
[25] A. Akelah, A. Rehab, T. Agag, M. Betiha, Polystyrene nanocomposite materials by *in situ* polymerization into montmorillonite–vinyl monomer interlayers, J. Appl. Polym. Sci. 103 (2007) 3739–3750.
[26] A. Legrouri, M. Lakraimi, A. Barroug, A.D. Roy, J.P. Besse, Removal of the herbicide 2,4-dichlorophenoxyacetate from water to zinc–aluminium–chloride layered double hydroxides, Water Res. 39 (2005) 3441–3448.
[27] A.A. Bakr, M.S. Mostafa, Gh. Eshaq, M.M. Kamel, Kinetics of uptake of Fe(II) from aqueous solutions by Co/Mo layered double hydroxide (Part 2), Desalin. Water Treat. 56 (2015) 248–255.
[28] M.A. Betiha, H.M.A. Hassan, A.M. Al-Sabagh, A.S. Khder, E.A. Ahmed, Direct synthesis and the morphological control of highly ordered mesoporous AlSBA-15 using urea-tetrachloroaluminate as a novel aluminum source, J. Mater. Chem. 22 (2012) 17551–17559.
[29] Z.M. Kheiralla, A.A. Rushdy, M.A. Betiha, N.A. Yakob, High-performance antibacterial of montmorillonite decorated with silver nanoparticles using microwave assisted method, J. Nanopart. Res. 16 (2014) 2560–2574.
[30] H.V. Olphen, J.J. Fripiat, Data Handbook for Clay Materials and Other Non-metallic Minerals, Pergamon, Oxford, 1979.
[31] D.Q. Pan, Q.H. Fan, P. Li, S.P. Liu, W.S. Wu, Sorption of Th(IV) on Na-bentonite: Effects of pH, ionic strength, humic substances and temperature, Chem. Eng. J. 172 (2011) 898–905.
[32] A. Mellah, S. Chegrouche, The removal of zinc from aqueous solutions by natural bentonite, Water Res. 31 (1997) 621–629.
[33] M.H. Al-Qunaibit, W.K. Mekhemer, A.A. Zaghloul, The adsorption of Cu(II) ions on bentonite—A kinetic study, J. Colloid Interfac Sci. 283 (2005) 316–321.
[34] S. Yariv, H. Cross (Eds.), Organo-clay Complexes and Interactions, Marcel Dekker, New York, NY, 2002.
[35] A.M.L. Kraepiel, K. Keller, F.M.M. Morel, A Model for metal adsorption on montmorillonite, J. Colloid Interface Sci. 210 (1999) 43–54.
[36] M.H. Bradbury, B. Baeyens, Modelling the sorption of Zn and Ni on Ca-montmorillonite, Geochim. Cosmochim. Acta 63 (1999) 325–336.
[37] B. Baeyens, M.H. Bradbury, A mechanistic description of Ni and Zn sorption on Na-montmorillonite Part I: Titration and sorption measurements, J. Contam. Hydrol. 27 (1997) 199–222.
[38] J. Ikhsan, J.D. Wells, B.B. Johnson, M.J. Angove, Surface complexation modeling of the sorption of Zn(II) by Montmorillonite, Colloids Surf., A: Physicochem. Eng. Aspects 252 (2005) 33–41.
[39] P. Stathi, K. Litina, D. Gournis, T.S. Giannopoulos, Y. Deligiannakis, Physicochemical study of novel organoclays as heavy metal ion adsorbents for environmental remediation, J. Colloid Interface Sci. 316 (2007) 298–309.